BIOCHEMISTRY
including biophysical chemistry & molecular biology

Article

pubs.acs.org/biochemistry

A Single Tyrosine Hydroxyl Group Almost Entirely Controls the NADPH Specificity of *Plasmodium falciparum* Ferredoxin-NADP$^+$ Reductase

Sara Baroni, Vittorio Pandini, Maria Antonietta Vanoni, and Alessandro Aliverti*

Department of Biomolecular Sciences and Biotechnology, Università degli Studi di Milano, via Celoria 26, 20133 Milano, Italy

ABSTRACT: *Plasmodium falciparum* ferredoxin-NADP$^+$ reductase (FNR) is a FAD-containing enzyme that, in addition to be a promising target of novel antimalarial drugs, represents an excellent model of plant-type FNRs. The cofactor specificity of FNRs depends on differences in both k_{cat} and K_m values for NADPH and NADH. Here, we report that deletion of the hydroxyl group of the conserved Y258 of *P. falciparum* FNR, which interacts with the 2′-phosphate group of NADPH, selectively decreased the k_{cat} of the NADPH-dependent reaction by a factor of 2 to match that of the NADH-dependent one. Rapid-reaction kinetics, active-site titrations with NADP$^+$, and anaerobic photoreduction experiments indicated that this effect may be the consequence of destabilization of the catalytically competent conformation of bound NADPH. Moreover, because the Y258F replacement increased the K_m for NADPH 4-fold and decreased that for NADH 3-fold, it led to a drop in the ability of the enzyme to discriminate between the coenzymes from 70- to just 1.5-fold. The impact of the Y258F change was not affected by the presence of the H286Q mutation, which is known to enhance the catalytic activity of the enzyme. Our data highlight the major role played by the Y258 hydroxyl group in determining the coenzyme specificity of *P. falciparum* FNR. From the general standpoint of engineering the kinetic properties of plant-type FNRs, although *P. falciparum* FNR is less strictly NADPH-dependent than its homologues, the almost complete abolishment of coenzyme selectivity reported here has never been accomplished before through a single mutation.

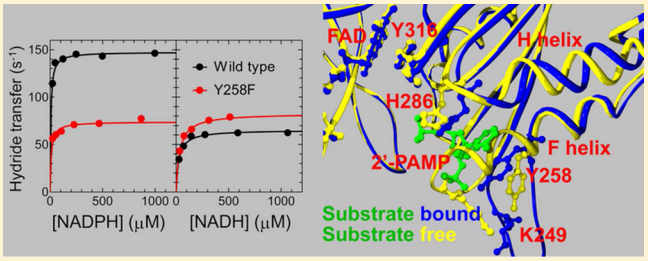

Plant-type ferredoxin-NADP$^+$ reductases (FNRs) are FAD-containing enzymes that catalyze the reversible exchange of reducing equivalents between the NADP$^+$/NADPH and the ferredoxin(Fe^{3+})/ferredoxin(Fe^{2+}) redox couples.[1−3] The prototype of FNRs is represented by the enzyme form responsible for NADPH regeneration in oxygenic photosynthesis. Whereas the strict relatives of the photosynthetic enzyme, the so-called "plastidic-type" FNRs, show remarkably similar properties, a divergent branch of plant-type FNRs, dubbed the "bacterial-type" FNRs, displays a greater variety of structural features, catalytic properties, and metabolic functions.[1] Furthermore, the structural module formed by the two-domain assembly of plant-type FNR has been recognized as the hallmark of the FNR protein superfamily,[4] which comprises enzymes that are highly medically relevant such as cytochrome P450 reductase,[5] Nox-family NADPH oxidases,[6] and nitric oxide synthases.[7]

Plastidic-type FNRs are usually highly specific for NADP$^+$ or NADPH [NADP(H)], displaying significantly higher values of both k_{cat}/K_m and k_{cat} for this coenzyme than for NAD$^+$ or NADH [NAD(H)].[2] The structural determinants of such coenzyme specificity have been extensively investigated, but a full understanding of the underlying mechanism(s) has not been developed. As expected, most of the difference in the binding energies of NADP(H) and NAD(H) relies on the specific interactions that FNR establishes with the 2′-phosphate group of the physiological coenzyme.[8] However, the FNR specificity significantly depends on k_{cat}, which is limited by the degree of access of the nicotinamide ring of the coenzyme to the active site, where hydride transfer (HT) between the nicotinamide and the flavin rings occurs.[2] Thus, other protein regions subtly affect discrimination against NAD(H). Such additional specificity determinants are amino acyl residues interacting with the substrate pyrophosphate group[9] and the C-terminal tyrosine, whose side chain functions as a gate to protect the *re* face of the flavin.[10,11]

In addition to higher plants, algae, and cyanobacteria, plastidic-type FNRs have been found in Apicomplexa,[12] a phylum of parasites that includes the malaria- and toxoplasmosis-causing agents, and in the bacterium *Leptospira interrogans*, which causes leptospirosis in humans and other mammals.[13] Apicomplexan FNR colocalizes with a plant-type ferredoxin in the apicoplast, a phylum-specific organelle, phylogenetically related to algal plastids. *Plasmodium falciparum* FNR (PfFNR) exhibits most of the basic features of typical plastidic FNRs but diverges from them by displaying a low turnover number and a much weaker ability to discriminate between NADPH and NADH.[14,15] These functional differences result from a few critical details in the way the plasmodial

Received: January 18, 2012
Revised: April 20, 2012
Published: April 20, 2012

dx.doi.org/10.1021/bi300078p | *Biochemistry* 2012, 51, 3819−3826

enzyme binds the 2′-phosphate group of NADPH.[14] The resulting peculiar interactions of PfFNR with the adenylate moiety of NADPH have been shown to be instrumental for the covalent dimerization of the enzyme under oxidizing conditions, which could be a physiological mechanism for turning off the enzyme activity in vivo.[15] Possibly, during the evolution of PfFNR, a trade-off has occurred between high specificity for the nicotinamide nucleotide substrate and a redox-based regulation mechanism. As a result, in PfFNR coenzyme specificity is controlled by a reduced set of enzyme−NADPH interactions as compared to those for other plastidic-type FNRs.[14] This greater simplicity makes PfFNR an ideal model for studying the events at the basis of NADP(H) recognition in the FNR protein family. Moreover, because this enzyme is a potentially excellent candidate as a target for novel antiplasmodial drugs,[16,17] a detailed understanding of its catalytic cycle is expected to contribute to the fight against malaria.

Here, we show that two PfFNR residues, namely, Y258 and H286, which interact with the 2′-phosphate and the pyrophosphate groups of NADPH, respectively (Figure 1),

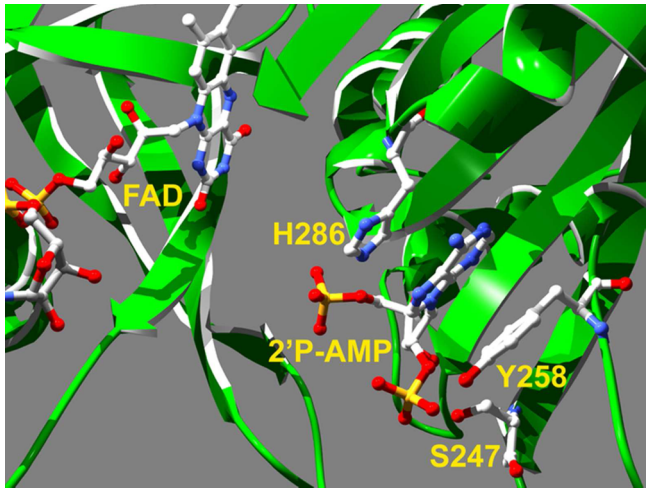

Figure 1. Three-dimensional structure of the PfFNR active site. Part of the cleft between the FAD-binding and NADP-binding domains is shown, with FAD, the substrate analogue adenosine 2′,5′-diphosphate (2′-PAMP), S247, Y258, and H286 represented as ball-and-stick models (PDB entry 2OK7, chain A). The distance between the oxygen atom of the Y258 side chain and the closest atom of the 2′-phosphate group of 2′-PAMP in the six protein molecules of the asymmetric unit has a mean value of 2.65 Å and a standard deviation of 0.13 Å.

have nonadditive roles in modulating the coenzyme specificity of this enzyme. Remarkably, removal of the Y258 hydroxyl group almost completely abolishes the ability of PfFNR to discriminate between NADPH and NADH, a result never accomplished before for any plant-type FNR through a single mutation.

MATERIALS AND METHODS

Materials. $NADP^+$, NADPH, and NADH were purchased from Sigma-Aldrich. All other chemicals were of the highest commercially available grade.

Site-Directed Mutagenesis. The base changes required for Y258F replacement were introduced into both pET-PfFNR[15] and pET-PfFNR-H286Q[18] using the QuikChange Lightning Site-Directed Mutagenesis Kit (Stratagene, Agilent Technologies Italia, Cernusco sul Naviglio, Milan, Italy) with the following pair of complementary mutagenic oligonucleotides (base changes underlined): 5′-TCAGATGCAACAAGTTTTT<u>TT</u>GTGCAAGATGAAATTTACAAAAGG-3′ and 5′-CCTTTTGTAAATTTCATCTTGCAC<u>AA</u>AAAAACTTGTTGCATCTGA-3′.

The resulting plasmids, carrying the single mutation and the double mutation, were named pET-PfFNR-Y258F and pET-PfFNR-Y258F/H286Q, respectively, and their inserts were fully sequenced to verify the presence of the desired base changes and to rule out unwanted mutations.

Protein Overproduction and Purification. Wild-type and mutant PfFNR forms were overproduced in *Escherichia coli* Rosetta(DE3) and purified as previously reported.[18]

Spectral Analyses. Absorption spectra were recorded on a model 8453 diode-array (Agilent Technologies Italia) or a double-beam Cary 100 (Varian, Agilent Technologies Italia) spectrophotometer. The extinction coefficients of the mutant PfFNRs were determined on the basis of the amount of FAD released following sodium dodecyl sulfate treatment.[19] Spectrophotometric active-site titrations with $NADP^+$ were conducted at 16 °C in 50 mM Tris-HCl (pH 7.6), as reported previously.[18] To determine the K_d values of the $NADP^+$ complexes of the PfFNR variants carrying the Y258F replacement, which yielded low-intensity spectral perturbation upon ligand binding, the first derivative of their difference spectra ($d\Delta A/d\lambda$) was calculated to substantially improve the signal-to-noise ratio. Anaerobic photoreduction of the FAD prosthetic group of PfFNR forms was performed with the deazariboflavin/EDTA system[20] at 15 °C. The enzymes were diluted to ∼15 μM in 50 mM HEPES-NaOH (pH 7.0) containing 10% glycerol, 15 mM EDTA, and 1.5 μM 5-carba-5-deazariboflavin. When present, $NADP^+$ was at a 1.2 molar ratio with respect to the enzyme.

Steady-State Kinetics. NADPH-dependent and NADH-dependent $K_3Fe(CN)_6$ activity assays were performed at 25 °C in 100 mM Tris-HCl (pH 8.2), as previously described.[18] To estimate the steady-state kinetic parameters of the enzyme forms, the concentrations of the electron donor (either NADPH or NADH) and of $K_3Fe(CN)_6$ were independently varied. All variants displayed a susceptibility to inhibition by the ferricyanide ion similar to that exhibited by the wild-type enzyme.[14] Because $K_3Fe(CN)_6$ was found to be saturating as a substrate at all concentrations tested, initial velocity data were fit to eq 1 by nonlinear regression analysis using GraFit version 5.0 (Erithacus Software Ltd., Horley, Surrey, U.K.):

$$v_0 = (k_{cat}[\text{PfFNR}]_T[\text{NAD(P)H}])/[(1+[I]/K_i)K_m + [\text{NAD(P)H}]] \quad (1)$$

where $[\text{PfFNR}]_T$ is the total concentration of the enzyme form considered, [NAD(P)H] is the concentration of either NADPH or NADH, which is considered the sole variable substrate, [I] represents the concentration of the competitive inhibitor $K_3Fe(CN)_6$, and K_i is the inhibition constant.

Rapid-Reaction Kinetics. Wild-type or mutant PfFNRs (17−19 μM, after mixing) were reacted with either NADPH or NADH (0.025−2 mM, after mixing) at 25 °C in 50 mM HEPES-NaOH (pH 7.0) under anaerobic conditions, using an SF-61 DX2 diode-array stopped-flow spectrophotometer (Hi-Tech Scientific, Bradford-upon-Avon, U.K.). For each shot, a set of 300 spectra within the 300−700 nm wavelength range was recorded over reaction times ranging from 0.5 to 7 s.

dx.doi.org/10.1021/bi300078p | *Biochemistry* 2012, 51, 3819−3826

Table 1. Steady-State Kinetic Parameters of the PfFNR Variants for the NADPH− and NADH−$K_3Fe(CN)_6$ Reductase Reactions[a]

PfFNR	k_{cat}^{NADPH}[b] (s^{-1})	K_m^{NADPH} (μM)	k_{cat}/K_m^{NADPH} ($s^{-1}\ \mu M^{-1}$)	k_{cat}^{NADH}[b] (s^{-1})	K_m^{NADH} (μM)	k_{cat}/K_m^{NADH} ($s^{-1}\ \mu M^{-1}$)	NADPH:NADH specificity ratio[c]
wild type	125 ± 4[d]	36 ± 6[d]	3.5 ± 0.5[d]	48 ± 2	720 ± 90	0.05 ± 0.005	70
H286Q	185 ± 3[d]	57 ± 5[d]	3.3 ± 0.3[d]	100 ± 3	715 ± 80	0.15 ± 0.015	22
Y258F	50 ± 0.5	160 ± 16	0.3 ± 0.03	47 ± 1	260 ± 40	0.2 ± 0.04	1.5
Y258F/H286Q	53 ± 0.5	240 ± 17	0.2 ± 0.01	47 ± 1	360 ± 40	0.15 ± 0.015	1.3

[a]The inhibitory effect of $K_3Fe(CN)_6$, which acts on PfFNR as a competitive inhibitor with respect to both NADPH and NADH,[14] was taken into account in the calculation of the kinetic parameters, as described in Materials and Methods. [b]k_{cat} values are expressed as moles of NADPH or NADH oxidized per mole of active site (FAD) per second. [c]Coenzyme specificity expressed as the ratio of k_{cat}/K_m^{NADPH} to k_{cat}/K_m^{NADH}. [d]Data taken from ref 18.

Absorbance traces were fit to exponential decay equations using KinetAsyst version 3.0 (Hi-Tech Scientific). In agreement with our previous report,[18] absorbance traces were biphasic, displaying the same rate constant values over the entire wavelength range considered. The slow phase, which accounted only for minor spectral changes, occurred at a rate that was independent of reductant concentration and was too low to represent a process involved in catalysis. The apparent rate constants of the fast phase (k_{app}) at different NADH or NADPH concentrations were calculated by averaging the values obtained by fitting the absorbance traces from at least three shots. To estimate the rate of HT (k_{HT}), the k_{app} values at different NADPH or NADH concentrations were fit to the equation of a hyperbole and its upper limit was extrapolated.

RESULTS AND DISCUSSION

The two PfFNR variants carrying either the single Y258F and double Y258F/H286Q replacement were synthesized in the bacterial host at levels comparable to that of the wild-type enzyme and were purified with similar yields, indicating that the Y258F mutation does not markedly affect the folding process or the stability of the native conformation of the protein. Similarly, the amino acyl replacement induced no alteration of the absorbance spectrum of the flavoenzyme, so that the same extinction coefficient of 10 $mM^{-1}\ cm^{-1}$ at 454 nm[14] could be used to quantify all the PfFNR forms studied here.

The reactivity toward NADPH of PfFNR variants carrying different replacements at position 286 was previously studied in detail and reported elsewhere.[18] Because that study indicated that H286 plays a role in orienting the NMN moiety during HT and because such a steering effect is known to affect coenzyme specificity in plastidic-type FNRs, we measured the NADH-dependent activity of the PfFNR-H286Q, PfFNR-H286K, PfFNR-H286A, and PfFNR-H286L variants, previously produced.[18] As expected, the specificity of all variants was significantly impaired with respect to that of the wild-type enzyme. However, only for PfFNR-H286Q could reliable kinetic data be obtained, the NADH-dependent activity of the other variants being too low for accurate measurements. As shown in Table 1, while the H286Q mutation hardly affected the K_m values for either NADPH or NADH, it significantly increased both k_{cat}^{NADPH} and k_{cat}^{NADH}. As a consequence of the stronger effect on k_{cat}^{NADH}, PfFNR-H286Q was found to be 3.2-fold less specific for the pyridine nucleotide than the wild-type enzyme. This result is in keeping with the previous report of a similar effect obtained by mutating the corresponding site in *Anabaena* FNR.[9] For these reasons, the contribution to the specificity of H286 was not further studied by the detailed analysis of additional H286 mutants.

NADPH/NADH specificity of PfFNR ultimately relies on interactions between the protein and the 2′-phosphate group of NADPH. Y258, which provides the second aromatic ring, in addition to H286, to sandwich the adenine moiety of the coenzyme, also donates a H-bond to the 2′-phosphate group of NADPH (Figure 1). Replacement of Y258 with a phenylalanine is expected to disrupt the latter interaction while leaving aromatic stacking unaffected. Thus, the Y258F substitution was introduced into both wild-type PfFNR and its H286Q variant. As shown in Table 1, the effect of the mutation on the steady-state kinetic parameters of PfFNR was largely independent of the presence of histidine or glutamine at position 286. In particular, the Y258F replacement abolished the difference between the k_{cat}^{NADPH} and k_{cat}^{NADH} of the single and double mutants, decreasing their k_{cat}^{NADPH} values to match almost exactly that of wild-type PfFNR for NADH. Furthermore, the Y258F mutation had opposite effects on K_m^{NADPH} and K_m^{NADH}, significantly increasing the former and lowering the latter. The combination of these effects led to a 50-fold decrease in the PfFNR specificity ratio, i.e., the ratio between the k_{cat}/K_m of each enzyme form for the two coenzymes, which dropped to a mere 1.3−1.5 (Table 1). Interestingly, the effect of H286Q and Y258F replacements displayed no additivity. Rather, the Y258F substitution fully abolished the enhancing effect the H286Q replacement had on the k_{cat} values of PfFNR.

Steady-state kinetic data (Table 1) suggested that the Y258 hydroxyl of PfFNR could have an important role in optimizing the HT from NADPH to FAD. This finding was not unexpected, because, as mentioned in the introductory section, the preference of plastidic-type FNRs for NADPH over NADH relies on both lower K_m and higher k_{cat} values for the former dinucleotide.[2,8] Because k_{cat} is related to the rate of HT between the nicotinamide nucleotide and the FAD prosthetic group in the enzyme−cofactor complex,[15] we studied in detail the reductive half-reaction of the enzyme forms by stopped-flow spectrophotometry, using both NADPH and NADH as the reductant. Experimental conditions matched those used in our previous studies of the reaction of PfFNR and its H286 mutants with NADPH,[15,18] allowing direct comparisons. Like other well-characterized members of plastidic-type FNRs,[2] the reaction of PfFNR with NADPH led to the formation of a charge-transfer complex (CT) between NADPH and FAD, which could be observed as an increase in the absorption above 550 nm, which was completed in the dead time of the instrument (2−3 ms). This process was followed by the bleaching of the flavin corresponding to the reduction of the prosthetic group, which occurred in a biphasic fashion. The fast phase, accounting for most of the total absorbance change, corresponds to HT; the slow one, which took place at a rate not

dx.doi.org/10.1021/bi300078p | *Biochemistry* 2012, 51, 3819−3826

compatible with catalysis, most probably represents a rearrangement of the reaction product.[18] Notably, a clear positive correlation between the extent of CT accumulation during the reaction of the various enzyme forms with NADPH and the k_{HT} value was observed.[18] In particular, PfFNR-H286Q displayed both an increased amount of transient CT formation and a higher k_{HT} for NADPH with respect to those of the wild-type enzyme (Figures 2 and 3). Here, we report for the first time the pre-steady-state characterization of the reaction of PfFNR forms with NADH. In agreement with steady-state data, the wild-type enzyme reacted with NADH showing a k_{HT} that is 44% of that determined with NADPH, with no significant CT formation (Figures 2 and 3 and Table 2). PfFNR-H286Q displayed a k_{HT} for NADH 2-fold higher than that of PfFNR, although such a large increase was not paralleled by formation of a significant amount of CT during the reaction. The Y258F mutation lowered the k_{HT} for NADPH to 50% of that of the wild type (Table 2) and abolished the accumulation of CT (Figures 2 and 3). Interestingly, the Y258F mutation did not hamper HT from NADH to FAD; on the contrary, it seemed to slightly increase the k_{HT} for NADH, in comparison to that of the wild-type enzyme (Table 2). The PfFNR-Y258F/H286Q double mutant displayed kinetic properties in all respects identical to those of PfFNR-Y258F (Figure 3 and Table 2), confirming that the effects of the Y258F replacement completely overshadow those of the H286Q one. As we showed elsewhere,[15] the k_{cat} of the NADPH–$K_3Fe(CN)_6$ reductase reaction catalyzed by PfFNR matches very well the k_{HT} value determined by stopped-flow spectrophotometry. Here we confirm that the turnover rate under saturating conditions is limited by the HT step, as shown by the nearly identical effects that the mutations introduced into PfFNR had on the k_{cat} and k_{HT} values of both NADPH- and NADH-dependent reactions (Tables 1 and 2).

Rapid-reaction kinetics strongly suggested that the decrease in the HT rate determined by Y258 hydroxyl deletion when NADPH, but not NADH, is the hydride donor might be the result of a specific destabilization of the catalytically competent conformation of bound NADPH, which in the wild-type and H286Q enzymes is associated with the transient formation of the CT between NADPH and FAD. To further confirm this conclusion, we subjected PfFNR-Y258F and PfFNR-Y258F/H286Q to anaerobic photoreduction in the absence and presence of $NADP^+$ in comparison with PfFNR and PfFNR-H286Q. In the absence of the ligand, the FAD prosthetic group of all PfFNR variants underwent reduction to the hydroquinone form in a similar fashion, with the accumulation of very small amounts of the FAD neutral semiquinone during the process (not shown). In the late stages of the photoreduction conducted in the presence of $NADP^+$, a long-wavelength absorbing species was observed in the case of the wild-type enzyme, representing a CT species (Figure 4A). We have previously shown that the amount of CT was slightly but significantly higher in the case of PfFNR-H286Q than in the case of the wild-type enzyme.[18] On the other hand, as clearly shown in panels B and C of Figure 4, no CT species were detected during the reduction of PfFNR-Y258F or PfFNR-Y258F/H286Q in the presence of $NADP^+$.

To further investigate the contribution of Y258 to substrate recognition, we studied the interaction of the PfFNR forms with $NADP^+$ by differential spectrophotometry. It is well-known that binding of $NADP^+$ to FNR perturbs the visible absorption spectrum of bound FAD,[10] and that the positive

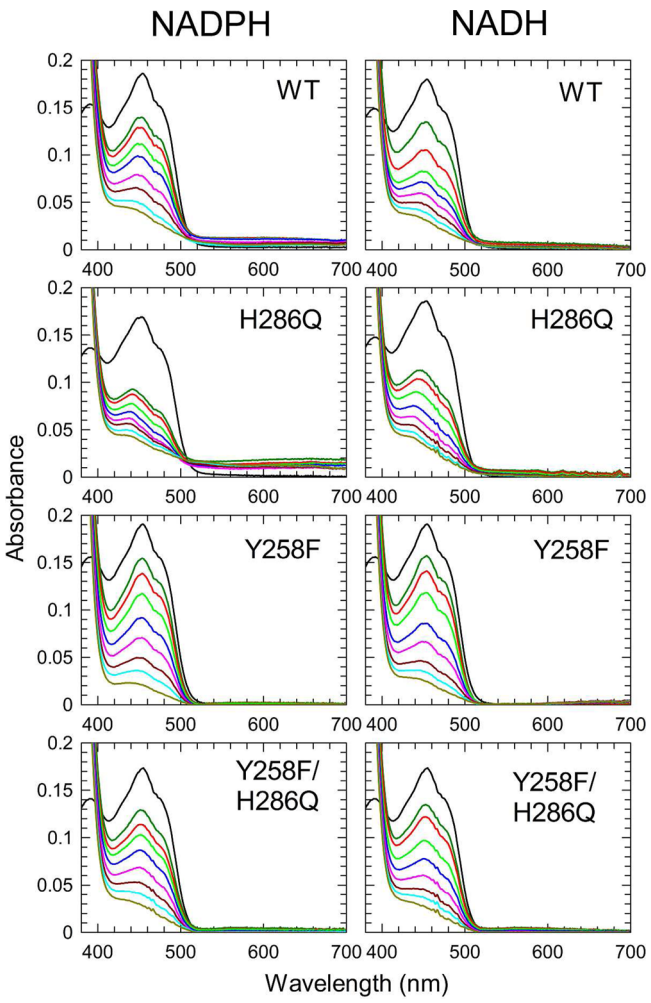

Figure 2. Spectra recorded by stopped-flow spectrophotometry during the anaerobic reduction of PfFNR forms by NADPH and NADH. PfFNR forms (17–19 μM) were reacted with 500 μM NADPH (left) or NADH (right) at 25 °C under anaerobiosis in 50 mM HEPES-NaOH (pH 7.0). In each panel, the spectrum of the oxidized PfFNR form is colored black while those recorded at increasing reaction times after mixing are depicted in different colors. NADPH: WT, 1 (dark green), 2 (red), 5 (light green), 7 (blue), 11 (magenta), 17 (brown), 61 (aqua), and 1000 ms (olive); H286Q, 0.74 (dark green), 2.2 (red), 3.7 (light green), 6.7 (blue), 11 (magenta), 32 (brown), 110 (aqua), and 450 ms (olive); Y258F, 1 (dark green), 3 (red), 7 (light green), 13 (blue), 21 (magenta), 41 (brown), 105 (aqua), and 600 ms (olive); Y258F/H286Q, 2 (dark green), 5 (red), 9 (light green), 15 (blue), 25 (magenta), 51 (brown), 165 (aqua), and 600 ms (olive). NADH: WT, 3 (dark green), 9 (red), 17 (light green), 23 (blue), 33 (magenta), 53 (brown), 115 (aqua), and 600 ms (olive); H286Q, 2 (dark green), 5 (red), 9 (light green), 19 (blue), 57 (magenta), 145 (brown), 275 (aqua), and 600 ms (olive); Y258F, 1 (dark green), 3 (red), 7 (light green), 15 (blue), 25 (magenta), 63 (brown), 155 (aqua), and 600 ms (olive); Y258F/H286Q, 1 (dark green), 3 (red), 9 (light green), 15 (blue), 25 (magenta), 51 (brown), 131 (aqua), and 600 ms (olive). Spectra of panels NADPH-WT and NADPH-H286Q are taken from ref 18 and are shown here for comparison.

peak around 500 nm in the difference spectrum (Figure 5A) is induced by the stacking between the $NADP^+$ nicotinamide and the FAD isoalloxazine.[11] Thus, the spectrophotometric titration of PfFNR with $NADP^+$ provides both the K_d of the resulting complex and a semiquantitative evaluation of the extent of occupancy of the enzyme active site by the nicotinamide ring of

dx.doi.org/10.1021/bi300078p | Biochemistry 2012, 51, 3819–3826

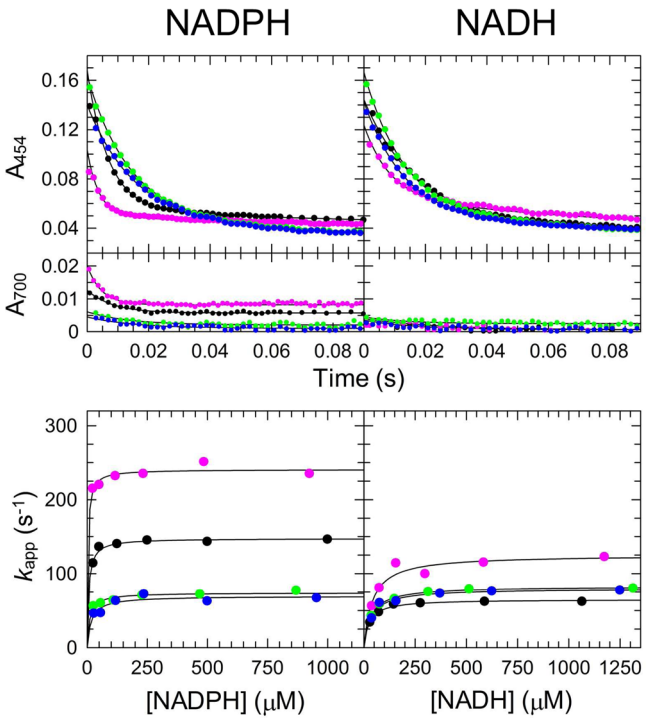

Figure 3. Time course and dependence by the concentration of NADPH and NADH of the reductive half-reaction of PfFNR forms, as studied by stopped-flow spectrophotometry. Enzyme forms (17−19 μM) were reacted at 25 °C, under anaerobiosis, in 50 mM HEPES-NaOH (pH 7.0) with NADPH and NADH at concentrations ranging from ≈25 μM to >1 mM after mixing. The top panels shows the absorbance at 454 and 700 nm recorded during the reaction of PfFNR (black), PfFNR-H286Q (magenta), PfFNR-Y258F (green), and PfFNR-Y258F/H286Q (blue) with NADPH (left) or NADH (right). The bottom panels show plots of the observed rate constant of the fast phase of the reaction (k_{app}) as a function of the concentration of NADPH (left) or NADH (right). Data from the four enzyme forms are reported in the same colors used in the top panels. Fitting the data sets with the equation of a rectangular hyperbola yielded the limit values for k_{app} (which provide the estimates of the corresponding k_{HT} values) reported in Table 2.

Table 2. Rate Constants of Hydride Transfer from NADPH and NADH to FAD in PfFNR Variants As Determined by Stopped-Flow Spectrophotometry

	k_{HT} (s^{-1})	
PfFNR form	NADPH	NADH
wild type	148 ± 2[a]	65 ± 1
H286Q	240 ± 4[a]	125 ± 7
Y258F	74 ± 2	83 ± 1
Y258F/H286Q	70 ± 4	80 ± 2

[a]Data taken from ref 18.

the ligand. As shown in Figure 5B, all mutant PfFNRs displayed a significantly lower affinity for $NADP^+$ in comparison to that of the wild-type protein, with the K_d values of the enzyme−$NADP^+$ complexes increased 2- or 3-fold (Table 3). More interestingly, as deduced from the comparison of the difference spectra displayed in Figure 5A and from the values of the differential extinction coefficient of the enzyme−$NADP^+$ complexes reported in Table 3, removal of the Y258 hydroxyl group highly destabilized the nicotinamide−flavin interaction. Such destabilization occurred even when the Y258F mutation

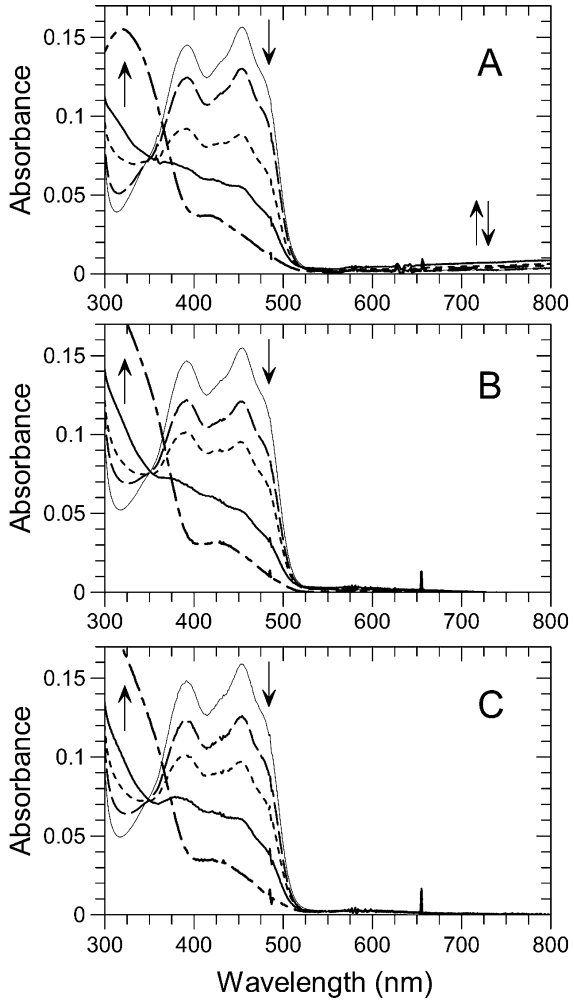

Figure 4. Anaerobic photoreduction of the FAD prosthetic group of PfFNR variants in the presence of $NADP^+$. Spectra of anaerobic mixtures of ≈15 μM PfFNR (A), PfFNR-Y258F (B), and PfFNR-Y258F/H286Q (C) in the presence of a slight excess of $NADP^+$ in 50 mM HEPES-NaOH (pH 7.0) recorded before (thin solid line) and after increasing irradiation times with visible light (different line styles). Arrows indicate the direction of the spectral changes observed during the experiment. Spectra were not corrected for the contribution of 5-deazariboflavin present in the mixtures.

was introduced into the PfFNR-H286Q variant, where the ring stacking interaction is stronger than in the case of PfFNR.

Taken as a whole, these data allow us to conclude that the Y258 side chain favors the adoption of the catalytically competent conformation of the NMN moiety of NADPH, enhancing HT and, therefore, enzyme turnover. In addition to productively interacting with NADPH, thus making it a good substrate, the side chain of Y258 also actively discriminates against NADH, by keeping K_m^{NADH} high. The structural basis of the latter effect can be rationalized considering that in the unbound PfFNR the side chain of Y258 is H-bonded to that of K249.[14] Whatever substrate is bound, either NADPH or NADH, this H-bond is severed because of the reported induced-fit reorganization of the substrate binding site.[14] However, while the binding energy lost by breaking the H-bond with K249 is compensated by the new interaction beween Y258 and NADPH, this compensation is not possible in the case of NADH, which lacks the 2′-phosphate group.

dx.doi.org/10.1021/bi300078p | *Biochemistry* 2012, 51, 3819−3826

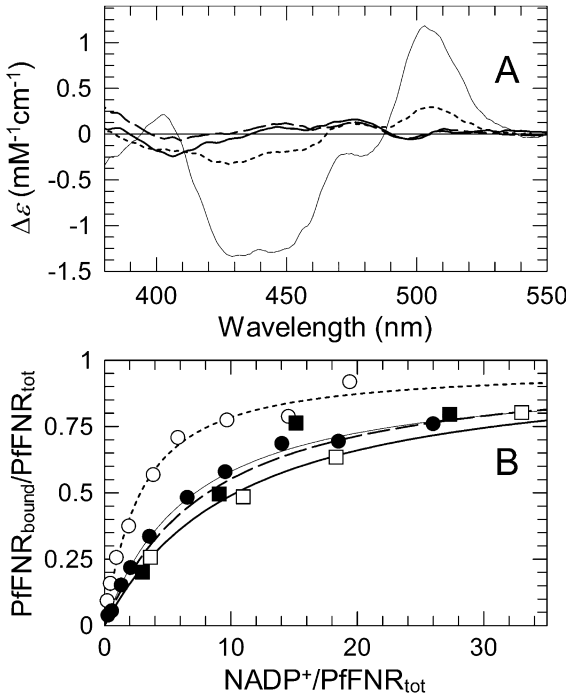

Figure 5. Binding of $NADP^+$ by PfFNR variants as studied by difference spectrophotometry. Spectrophotometric titrations of PfFNR forms with $NADP^+$ in 50 mM Tris-HCl (pH 7.6) at 15 °C. Data for the titrations of PfFNR and PfFNR-H286Q were taken from ref 17 and are displayed for comparison. (A) Difference spectra of enzyme–$NADP^+$ complexes computed by extrapolation to infinite $NADP^+$ concentration, for PfFNR (dotted line), PfFNR-H286Q (thin solid line), PfFNR-Y258F (thick solid line), and PfFNR-Y258F/H286Q (dashed line). (B) Progress of the titration of PfFNR (○), PfFNR-H286Q (●), PfFNR-Y258F (□), and PfFNR-Y258F/H286Q (■). Each curve was obtained by nonlinear fitting of the data with the theoretical equation for 1:1 binding.

Table 3. Dissociation Constants of the Complexes between the PfFNR Variants and $NADP^+$ and Intensities of the Ligand-Induced Spectral Perturbation of Bound FAD

PfFNR form	K_d (μM)	$\Delta\varepsilon_{508}$ (mM^{-1} cm^{-1})
wild type	60 ± 9[a]	0.30 ± 0.01
H286Q	130 ± 10[a]	1.14 ± 0.04
Y258F	170 ± 30	0.04 ± 0.002
Y258F/H286Q	130 ± 40	0.03 ± 0.002

[a]Data taken from ref 18.

What is the possible structural explanation of the effect of the interaction between PfFNR Y258 and NADPH 2′-phosphate on k_{cat}^{NADPH}? As in the other plastidic-type FNRs, PfFNR mainly interacts with the adenylate moiety of NADP(H). Indeed, the adenine, the 2′-phosphate, and the 5′-phosphate groups provide most contact sites.[2] The overlay of the crystal structures of ligand-free and 2′-PAMP-bound PfFNR displayed in Figure 6 clearly shows that the binding of this ligand, which mimics the adenylate half of the coenzyme, in addition to determining the unfolding of two turns of the αF helix, induces a large (2 Å) shift of the αH helix (residues 288–298), which moves away from FAD.[14] The N-terminal side of αH helix points toward the carboxylate of the C-terminal Y316, whose side chain stacks onto the *re* face of the flavin ring. Therefore, it is conceivable that the helix shift relieves some steric pressure from the latter residue, favoring the displacement of its phenolic side chain by

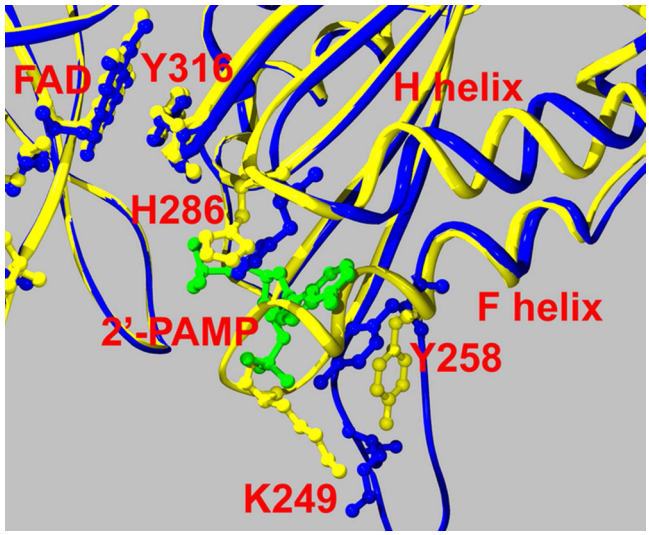

Figure 6. Induced-fit conformational changes induced by binding of 2′-PAMP to PfFNR. The crystal structures of ligand-free (PDB entry 2OK8, chain A) and 2′-PAMP-bound (PDB entry 2OK7, chain A) PfFNR are colored yellow and blue, respectively. Relevant amino acyl residues and ligands are represented as ball-and-stick models. 2′-PAMP is colored green.

the incoming nicotinamide ring of the bound coenzyme. H286 is located at a strategic site (i.e., in the loop connecting the β10 strand to the αH helix) to drive such helix movement when NADPH occupies its binding site. In our hypothesis, the adenylate moiety of the substrate acts as a lever on the αH helix: when the 2′-phosphate group of the ligand is anchored to the S247 and Y258 side chains, the interactions of the 5′-phosphate and adenine groups with H286 induce the above-described αH helix shift, which allows the nicotinamide ring of the coenzyme to access the active site.

The PfFNR specificity ratio of 70 (Table 1) is orders of magnitude lower than the corresponding value of 180000, reported for its homologue of *Toxoplasma gondii*,[21] a parasite related to *Plasmodium*. Thus, it is worth discussing the possible reasons for the poor selectivity of PfFNR for NADPH. As we previously reported, an obvious structural basis for the limited specificity of PfFNR is the lack of positively charged side chains interacting with the 2′-phosphate group of NADPH.[14] We have also shown that PfFNR undergoes a $NADP^+$-triggered dimerization process that results in enzyme inactivation in the presence of oxidizing agents, such as H_2O_2, which lock the homodimer via the formation of an intersubunit disulfide bridge.[15] The formation of the inactive homodimer is favored by NADP(H) binding in two ways, namely, (i) by promoting the unfolding of the αF helix in each subunit, which removes a major steric obstacle to dimerization, and (ii) by leading to the formation of two ionic interactions between the 2′-phosphate of the ligand molecules and the side chains of K287 and K292 of each opposite subunit.[14] The absence of ionic bonds involving the 2′-phosphate within the same subunit is thus functional to the inactivation process, where two NADP(H) molecules are sandwiched at the intersubunit interface of the dimer.[14] The low coenzyme specificity of PfFNR in comparison to those of its orthologs may well be due to specific metabolic features of the plasmodial apicoplast. Unfortunately, the actual concentrations of NADH and NADPH in the organelle are not available, and although some plasmodial apicoplast enzymes are thought to be highly NADH- or NADPH-specific,[22−24] a

dx.doi.org/10.1021/bi300078p | *Biochemistry* 2012, 51, 3819–3826

comprehensive kinetic characterization with both coenzymes has been reported for none of them. In the absence of more convincing explanations, it is tempting to hypothesize that the loss of specificity might represent the price paid by PfFNR to gain a regulation mechanism of its catalytic activity. The rationale behind the ability of PfFNR to be turned off by oxidants could reside in the need for the parasite to save NADPH to cope with reactive oxygen species under oxidative stress conditions.[25]

CONCLUSION

Through the interpretation of our results in light of the crystal structure of PfFNR, we have provided a sound picture of the structural bases of the coenzyme specificity of this enzyme. The obvious question is whether this model can be extended to interpret coenzyme specificity in the other plastidic-type FNRs. At first glance, the answer is negative. Indeed, PfFNR is the only member of this group of enzymes known to undergo a large conformational change upon coenzyme binding.[2] Furthermore, H286 is not conserved in nonplasmodial FNRs. However, the bulky, aliphatic residue that in other plastidic-type FNRs replaces it (usually a leucine) similarly interacts with the adenine moiety of the ligand and contributes to coenzyme specificity.[9] In pea leaf FNR, it has been experimentally shown that binding of 2′-PAMP, which mimics the NADP(H) adenylate moiety, favors the interaction of analogues of the nicotinamide ring with the active site.[26] This induced-fit effect has been proposed to be mediated by a conformational transition involving the loop that in PfFNR includes C284, G285, and H286, which is in contact with the C-terminal tyrosine that controls access to the active site.[26] Small conformational changes in this loop have actually been observed in *Anabaena* FNR upon $NADP^+$ binding by X-ray crystallography.[27] Moreover, the comparison among free and $NADP^+$-bound forms of *Anabaena* FNR (PDB entries 1QUE, 1QUF, and 1GJR)[27] shows that binding of $NADP^+$ (resulting in complexes where the adenylate moiety occupies the expected binding site, but the NMN portion of the ligand adopts conformations incompatible with HT) also induces small rearrangements also in the 267−279 α helix, which corresponds to the αH helix of PfFNR. A similar comparison between the crystal structures of free (PDB entry 1FNB) and 2′-PAMP-bound (PDB entry 1FND) spinach leaf FNR[28] shows that also in this protein ligand binding induces a small 0.3−0.4 Å shift in the same α helix (residues 276−290). Thus, although this phenomenon is particularly marked in the case of PfFNR, our results strongly support the notion that the k_{cat} component of the coenzyme specificity of plastidic-type FNRs is based on induced-fit conformational changes of variable extents, in which structural alterations of the loop that includes H286 and the shift of the α helix pointing toward the C-terminus of the protein play a significant role.

AUTHOR INFORMATION

Corresponding Author

*Department of Biomolecular Sciences and Biotechnology, Università degli Studi di Milano, via Celoria 26, 20133 Milano, Italy. Phone: +39 02 50314897. Fax: +39 02 50314895. E-mail: alessandro.aliverti@unimi.it.

Notes

The authors declare no competing financial interest.

ACKNOWLEDGMENTS

We are grateful to Dr. Laura Marangoni for valuable technical assistance in performing some of the experiments here reported.

ABBREVIATIONS

FNR, ferredoxin-$NADP^+$ reductase (EC 1.18.1.2); NADP(H), $NADP^+$ or NADPH; NAD(H), NAD^+ or NADH; HT, hydride transfer; PfFNR, *P. falciparum* FNR; 2′-PAMP, adenosine 2′,5′-diphosphate; k_{app}, apparent first-order rate constant; k_{HT}, rate constant of HT; NMN, nicotinamide mononucleotide; CT, charge-transfer complex; PDB, Protein Data Bank.

REFERENCES

(1) Ceccarelli, E. A., Arakaki, A. K., Cortez, N., and Carrillo, N. (2004) Functional plasticity and catalytic efficiency in plant and bacterial ferredoxin-NADP(H) reductases. *Biochim. Biophys. Acta 1698*, 155−165.

(2) Aliverti, A., Pandini, V., Pennati, A., de Rosa, M., and Zanetti, G. (2008) Structural and functional diversity of ferredoxin-$NADP^+$ reductases. *Arch. Biochem. Biophys. 474*, 283−291.

(3) Medina, M. (2009) Structural and mechanistic aspects of flavoproteins: Photosynthetic electron transfer from photosystem I to $NADP^+$. *FEBS J. 276*, 3942−3958.

(4) Karplus, P. A., Daniels, M. J., and Herriott, J. R. (1991) Atomic structure of ferredoxin-$NADP^+$ reductase: Prototype for a structurally novel flavoenzyme family. *Science 251*, 60−66.

(5) Laursen, T., Jensen, K., and Møller, B. L. (2011) Conformational changes of the NADPH-dependent cytochrome P450 reductase in the course of electron transfer to cytochromes P450. *Biochim. Biophys. Acta 1814*, 132−138.

(6) Sumimoto, H. (2008) Structure, regulation and evolution of Nox-family NADPH oxidases that produce reactive oxygen species. *FEBS J. 275*, 3249−3277.

(7) Stuehr, D. J., Tejero, J., and Haque, M. M. (2009) Structural and mechanistic aspects of flavoproteins: Electron transfer through the nitric oxide synthase flavoprotein domain. *FEBS J. 276*, 3959−3974.

(8) Medina, M., Luquita, A., Tejero, J., Hermoso, J., Mayoral, T., Sanz-Aparicio, J., Grever, K., and Gomez-Moreno, C. (2001) Probing the determinants of coenzyme specificity in ferredoxin-$NADP^+$ reductase by site-directed mutagenesis. *J. Biol. Chem. 276*, 11902−11912.

(9) Tejero, J., Martínez-Julvez, M., Mayoral, T., Luquita, A., Sanz-Aparicio, J., Hermoso, J. A., Hurley, J. K., Tollin, G., Gómez-Moreno, C., and Medina, M. (2003) Involvement of the pyrophosphate and the 2′-phosphate binding regions of ferredoxin-$NADP^+$ reductase in coenzyme specificity. *J. Biol. Chem. 278*, 49203−49214.

(10) Deng, Z., Aliverti, A., Zanetti, G., Arakaki, A. K., Ottado, J., Orellano, E. G., Calcaterra, N. B., Ceccarelli, E. A., Carrillo, N., and Karplus, P. A. (1999) A productive $NADP^+$ binding mode of ferredoxin-$NADP^+$ reductase revealed by protein engineering and crystallographic studies. *Nat. Struct. Biol. 6*, 847−853.

(11) Piubelli, L., Aliverti, A., Arakaki, A. K., Carrillo, N., Ceccarelli, E. A., Karplus, P. A., and Zanetti, G. (2000) Competition between C-terminal tyrosine and nicotinamide modulates pyridine nucleotide affinity and specificity in plant ferredoxin-$NADP^+$ reductase. *J. Biol. Chem. 275*, 10472−10476.

(12) Vollmer, M., Thomsen, N., Wiek, S., and Seeber, F. (2001) Apicomplexan parasites possess distinct nuclear-encoded, but apicoplast-localized, plant-type ferredoxin-$NADP^+$ reductase and ferredoxin. *J. Biol. Chem. 276*, 5483−5490.

(13) Nascimento, A. S., Catalano-Dupuy, D. L., Bernardes, A., de Oliveira Neto, M., Santos, M. A., Ceccarelli, E. A., and Polikarpov, I. (2007) Crystal structures of *Leptospira interrogans* FAD-containing ferredoxin-$NADP^+$ reductase and its complex with $NADP^+$. *BMC Struct. Biol. 7*, 69.

(14) Milani, M., Balconi, E., Aliverti, A., Mastrangelo, E., Seeber, F., Bolognesi, M., and Zanetti, G. (2007) Ferredoxin-NADP$^+$ reductase from *Plasmodium falciparum* undergoes NADP$^+$-dependent dimerization and inactivation: Functional and crystallographic analysis. *J. Mol. Biol. 367*, 501−513.
(15) Balconi, E., Pennati, A., Crobu, D., Pandini, V., Cerutti, R., Zanetti, G., and Aliverti, A. (2009) The ferredoxin-NADP$^+$ reductase/ferredoxin electron transfer system of *Plasmodium falciparum*. *FEBS J. 276*, 3825−3836.
(16) Röhrich, R. C., Englert, N., Troschke, K., Reichenberg, A., Hintz, M., Seeber, F., Balconi, E., Aliverti, A., Zanetti, G., Köhler, U., Pfeiffer, M., Beck, E., Jomaa, H., and Wiesner, J. (2005) Reconstitution of an apicoplast-localised electron transfer pathway involved in the isoprenoid biosynthesis of *Plasmodium falciparum*. *FEBS Lett. 579*, 6433−648.
(17) Seeber, F., Aliverti, A., and Zanetti, G. (2005) The plant-type ferredoxin-NADP$^+$ reductase/ferredoxin redox system as a possible drug target against apicomplexan human parasites. *Curr. Pharm. Des. 11*, 3159−3172.
(18) Crobu, D., Canevari, G., Milani, M., Pandini, V., Vanoni, M. A., Bolognesi, M., Zanetti, G., and Aliverti, A. (2009) *Plasmodium falciparum* ferredoxin-NADP$^+$ reductase His286 plays a dual role in NADP(H) binding and catalysis. *Biochemistry 48*, 9525−9533.
(19) Aliverti, A., Curti, B., and Vanoni, M. A. (1999) Identifying and quantitating FAD and FMN in simple and in iron-sulfur-containing flavoproteins. *Methods Mol. Biol. 131*, 9−23.
(20) Massey, V., and Hemmerich, P. (1977) A photochemical procedure for reduction of oxidation-reduction proteins employing deazariboflavin as catalyst. *J. Biol. Chem. 252*, 5612−5614.
(21) Pandini, V., Caprini, G., Thomsen, N., Aliverti, A., Seeber, F., and Zanetti, G. (2002) Ferredoxin-NADP$^+$ reductase and ferredoxin of the protozoan parasite *Toxoplasma gondii* interact productively *in vitro* and *in vivo*. *J. Biol. Chem. 277*, 48463−48471.
(22) Krauth-Siegel, R. L., Müller, J. G., Lottspeich, F., and Schirmer, R. H. (1996) Glutathione reductase and glutamate dehydrogenase of *Plasmodium falciparum*, the causative agent of tropical malaria. *Eur. J. Biochem. 235*, 345−350.
(23) Kapoor, M., Dar, M. J., Surolia, A., and Surolia, N. (2001) Kinetic determinants of the interaction of enoyl-ACP reductase from *Plasmodium falciparum* with its substrates and inhibitors. *Biochem. Biophys. Res. Commun. 289*, 832−837.
(24) Pillai, S., Rajagopal, C., Kapoor, M., Kumar, G., Gupta, A., and Surolia, N. (2003) Functional characterization of β-ketoacyl-ACP reductase (FabG) from *Plasmodium falciparum*. *Biochem. Biophys. Res. Commun. 303*, 387−392.
(25) Kehr, S., Sturm, N., Rahlfs, S., Przyborski, J. M., and Becker, K. (2010) Compartmentation of redox metabolism in malaria parasites. *PLoS Pathog. 6*, e1001242.
(26) Paladini, D. H., Musumeci, M. A., Carrillo, N., and Ceccarelli, E. A. (2009) Induced fit and equilibrium dynamics for high catalytic efficiency in ferredoxin-NADP(H) reductases. *Biochemistry 48*, 5760−5768.
(27) Hermoso, J. A., Mayoral, T., Faro, M., Gómez-Moreno, C., Sanz-Aparicio, J., and Medina, M. (2002) Mechanism of coenzyme recognition and binding revealed by crystal structure analysis of ferredoxin-NADP$^+$ reductase complexed with NADP. *J. Mol. Biol. 319*, 1133−1142.
(28) Bruns, C., and Karplus, P. A. (1995) Refined crystal structure of spinach ferredoxin reductase at 1.7 Å resolution: Oxidized, reduced and 2′-phospho-5′-AMP bound states. *J. Mol. Biol. 247*, 125−145.